ORIGINAL ARTICLE

Radon detector development using a PIN photodiode

Lorenzo Visca[1]*, Antonio Amoroso[1], Roberta Calabria[1], Giorgio Cotto[1], Aldo Crosetto[2], Marco Giovanni Maria Destefanis[1], Elisabetta Alessandra Durisi[1], Francesco Mallamace[1], Pier Paolo Trapani[2] and Lorenzo Zamprotta[1]

[1]Physics Department of the University of Torino, Torino, Italy; [2]External Collaborator, Torino, Italy

Abstract

An active device for radon detection in air has been developed in the frame of a project carried out by the Physics Department of the University of Torino with the aim to create a monitoring network of radon concentration in the University workplaces.
The device uses a commercial planar photodiode, sensitive to alpha particles, and a dedicated electronic chain integrated in an approx. 30 mm by 50 mm printed circuit board (PCB), designed in order to minimize the power consumption. The device can be used not only as alpha particles counter (using the digital output) but also for alpha spectroscopy, connecting the analog signal output from the shaper amplifier to a Multichannel Analyzer (MCA).
In this paper, the first prototype of the detector will be presented with the preliminary experimental results.
The spectroscopic performances of the device were tested, integrating the sensor in a commercial aluminum box and acquiring the alpha particle spectrum from a calibration source and from rock samples used as radon sources.
The radon sensitivity of the detector, in terms of (Counts per hour)/(Bq m^{-3}), was assessed by the comparison with a calibrated commercial radon detector (RAD7 Durridge Inc.).
In conclusion, the final prototype will be presented. It is characterized by a new 3d printed plastic case in black PA12 for light shielding, covered by a conductive paint in order to minimize the electromagnetic noise.

Keywords: *silicon photodiode; alpha spectroscopy; continuous radon monitor; radon device intercomparison; radon network*

Radon is a radioactive natural gas belonging to the class of noble gases. Different isotopes of radon exist, but the most significant one (for human exposure), due to its long half-life time (3.82 days), is ^{222}Rn (1). It derives from alpha decay from the ^{238}U series. This nuclide is present in various concentrations in all soils and rocks (2), making the soil the primary source of atmospheric radon. Radon exhaled outdoors disperses quickly (3). On the other hand, in closed environments (indoor), the radon tends to accumulate, sometimes reaching indoor concentration levels representing a risk to human health. More precisely, radon represents one of the primary risk factors of lung cancer, classified from the World Health Organization (WHO) through the International Agency for Research on Cancer (IARC) in the first group of carcinogens (4). The lung cancer risk is proportional to the radon exposure (5); therefore, it is crucial to measure radon concentration.

There are several devices for measuring radon concentration in air. However, the device choice varies according to the measurement purpose (e.g. workplace monitoring (6) or verification of the effectiveness of the remedial action).

This paper presents a continuous radon monitor based on a Si PIN photodiode. The instrument has been developed at the Physics Department of the University of Torino with the aim to create a monitoring network.

The alpha particles detection works on counting the electric signals produced by the interaction between the particles themselves and the sensitive region of a photodiode. Therefore, the device is able to detect alpha particles coming directly from the ^{222}Rn and from its decay products (^{218}Po and ^{214}Po).

This document presents the device characterization and the preliminary measurements of radon concentration. These were performed at Physics Department of the University of Torino using natural rock samples as radon sources. Measurements were carried out simultaneously with a calibrated commercial device (RAD7 Durridge Inc.) (7).

Journal of the European Radon Association 2023. © 2023 Lorenzo Visca et al. This is an Open Access article distributed under the terms of the Creative Commons Attribution-NonCommercial4.0 International License (http://creativecommons.org/licenses/by-nc/4.0/), permitting all non-commercial use, distribution, and reproduction in any medium, provided the original work is properly cited.

Material and methods

The system consists of several parts (Fig. 1): the photodiode detector, a voltage multiplier for detector polarization, a preamplifier, a shaping amplifier, a second amplification – buffer stage, and, finally, a signal discriminator.

The sensitive element is a windowless Si PIN photodiode S3590-09 with a photosensitive area of 10 × 10 mm^2 by Hamamatsu (8–10). The following features make such photodiode particularly suitable for our application:

- maximum reverse voltage of 100 V;
- a terminal capacitance of 40 pF;
- high stability and good energy resolution.

The photodiode according to the characteristics mentioned above is polarized with 30 V using a Cockcroft-Walton voltage multiplier. Both the voltage multiplier and the electronic circuit use SMD CMOS low-power components. In this way, the device can be powered with only three 1.5 V AA batteries allowing to operate it without a bench power supply.

During the interaction between a charged particle and the photodiode sensitive area, a current proportional to the deposited energy is generated. Then, the current signal is transformed into a voltage signal by means of a charge to voltage preamplifier. Consequently, the shaping amplifier converts the voltage signal into a Gaussian pulse. This

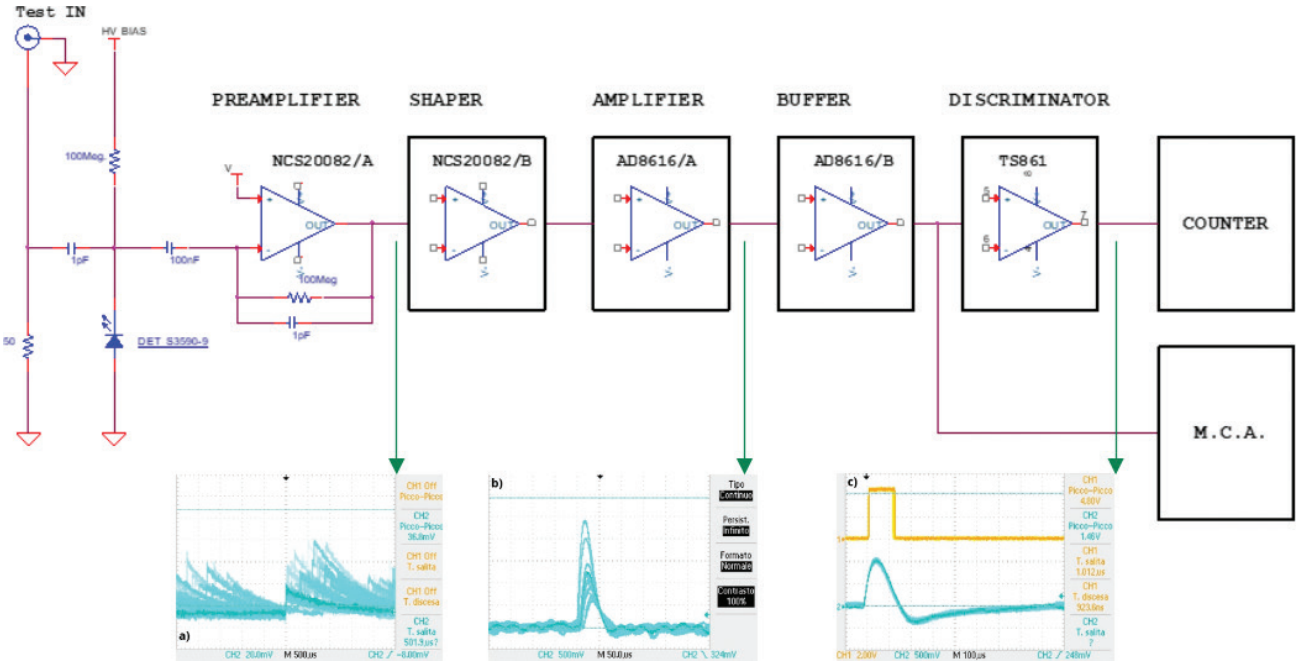

Fig. 1. Diagram of the detection system and acquired signals using the oscilloscope.

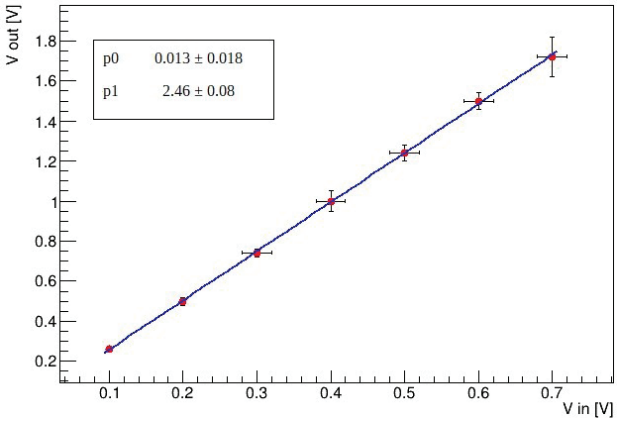

Fig. 2. Electronic chain linearity.

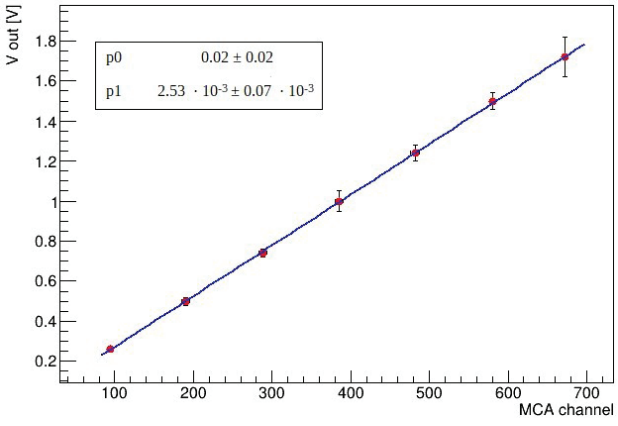

Fig. 3. Multichannel linearity.

Citation: Journal of the European Radon Association 2023, **4**: 8860 http://dx.doi.org/10.35815/radon.v4.8860

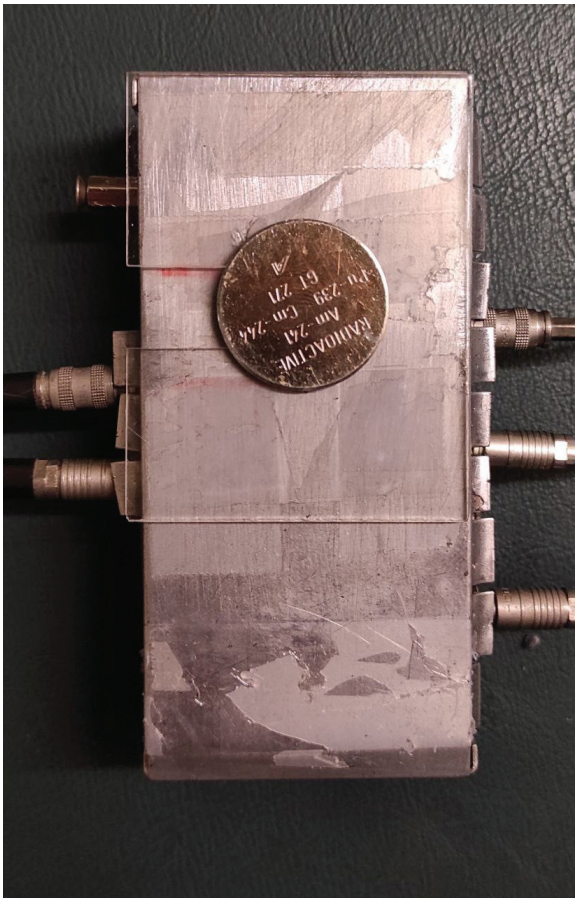

Fig. 4. Calibration setup using alpha source.

signal is internally processed by a discriminator, which generates a digital output for an external counter, and, once buffered, it can be sent to an Multichannel Analyzer (MCA) for alpha spectrum acquisition. The presence of a test-in input allows to test the device using a pulse generator.

Results

Linearity of the electronic chain

The electronic chain linearity was assessed using test-in signals from a pulse generator. Data are shown in Fig. 2 together with linear regression result. The analogue signal (V out) can be digitalized using an MCA in order to measure the particle energy spectrum. Figure 3 displays the results of the linearity of the digitalization process using Amptek MCA 8000A (11).

Test with a calibrated alpha source

In order to verify the spectroscopic performances of the system, preliminary tests were carried out acquiring the

Table 1. Correspondence between incoming particles' energy and MCA channels

Alpha emitter	Energy [MeV]	Energy after (0.93 ± 0.03) cm air [MeV]	Peak centroid [Channel]	σ [Channel]
^{239}Pu	5.16	4.31 ± 0.03	169	6
^{241}Am	5.49	4.68 ± 0.03	187	5
^{244}Cm	5.81	5.03 ± 0.03	202	5

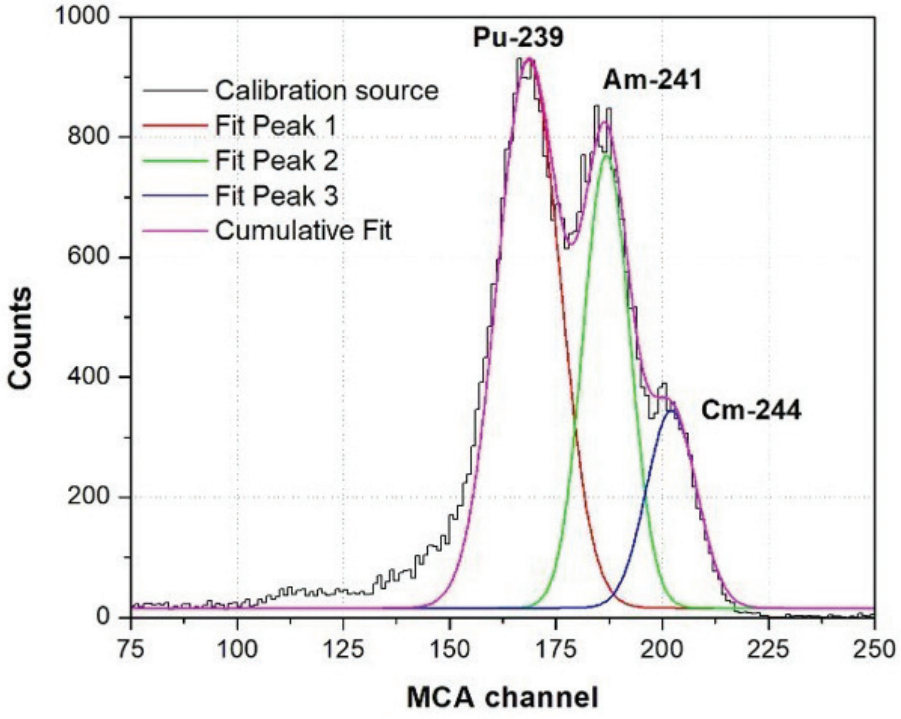

Fig. 5. Alpha spectrum of the calibration source acquired with the first prototype.

alpha spectrum coming from a composite alpha source (^{241}Am-^{244}Cm-^{239}Pu). The source, unsealed radioactive source type VZ-1679, shows a first maximum energy peak at 5.16 MeV (^{239}Pu), a second energy peak at 5.49 MeV (^{241}Am), and a third peak at 5.81 MeV (^{244}Cm) (12). The activities calculated at measurement data are, respectively, 1 kBq for ^{241}Am, 0.5 kBq for ^{244}Cm, and 1 kBq for ^{239}Pu.

The detector was assembled into an 8 × 5 × 2.5 cm^3 aluminum box. As it is shown in Fig. 4, the calibration source was placed on a plastic holder located directly on the aluminum cover; both the holder and the cover were specifically drilled in correspondence of the photodiode sensitive area. The air gap between the source and the photodiode has been measured using a callipers with a

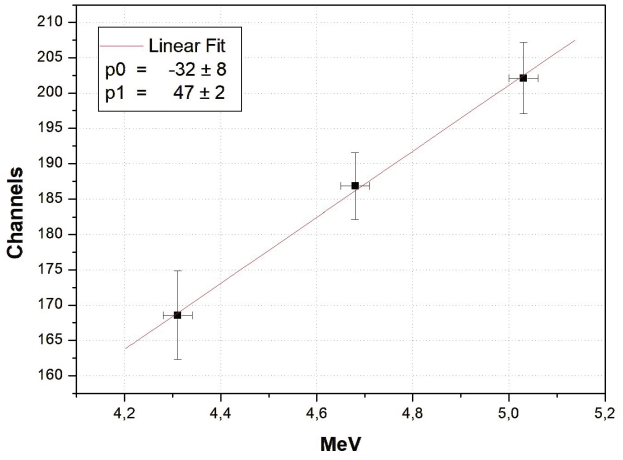

Fig. 6. Channels versus alpha energy.

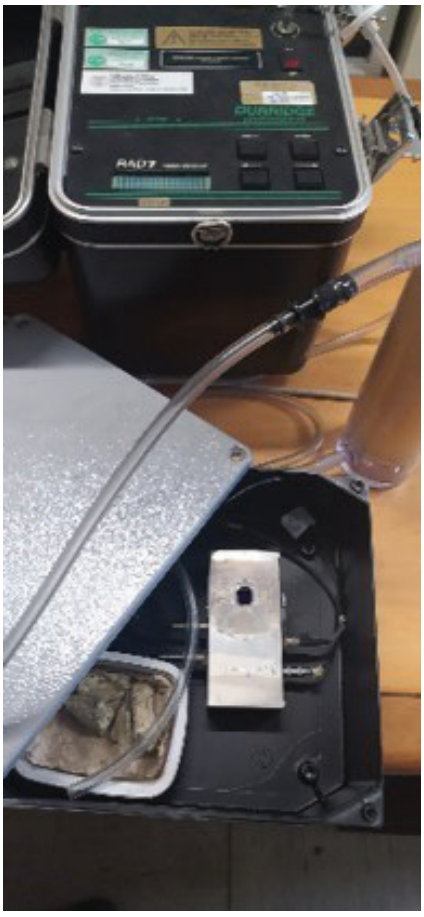

Fig. 8. Experimental setup with the prototype, the rock samples, and the tube of RAD7 inside the light-tight metal box.

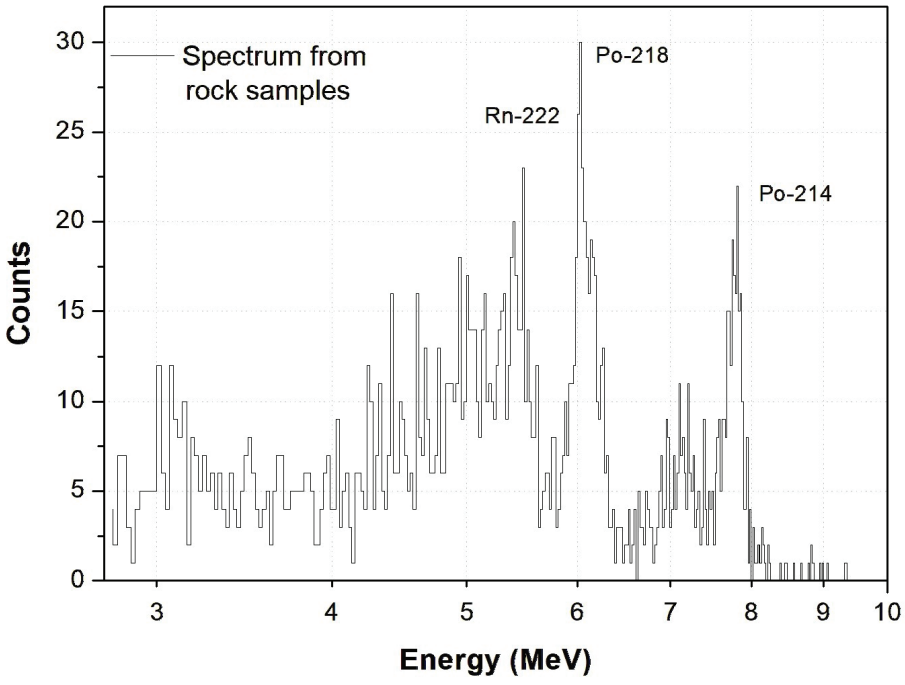

Fig. 7. Radon spectrum acquired from rock samples with first prototype.

Citation: Journal of the European Radon Association 2023, **4**: 8860 http://dx.doi.org/10.35815/radon.v4.8860

sensitivity of 0.05 mm. Taking into account the distance between the photodiode and the box surface of 7.10 mm, the source plate thickness of 2.20 mm, the uncertainty in the callipers positioning, and the uncertainty due to the source thickness, the air gap has been assessed 9.3 ± 0.3 mm. Both the aluminum box and the source were placed into a 25 × 22 × 8 cm^3 light-tight metal box to reduce the light noise. Figure 5 shows the spectrum acquired for 300 s, and the data are summarized in Table 1. The energy values after the air gap have been computed considering the mean energy loss in the dry air extrapolated from NIST data (13). The associated uncertainties are calculated considering the uncertainty on air thickness. As it can be noticed, the resolution in air (calculated as 2.35 ·σ/Peak centroid) is below 10%. Figure 6 displays the correspondence between the MCA channels and the incoming particles' energy, along with the linear regression.

Table 2. Measurements obtained with the first prototype and the RAD7 in three different experimental conditions (cph vs. Bq m^{-3})

Radon concentration	Time [s]	Count rates above the threshold [cph]	σ [cph]	RAD7 [Bq m^{-3}]	σ [Bq m^{-3}]
Conc 1	86,400	1.46	0.25	122	13
Conc 2	341,873	5.28	0.25	550	11
Conc 3	234,000	27.92	0.66	3,019	63

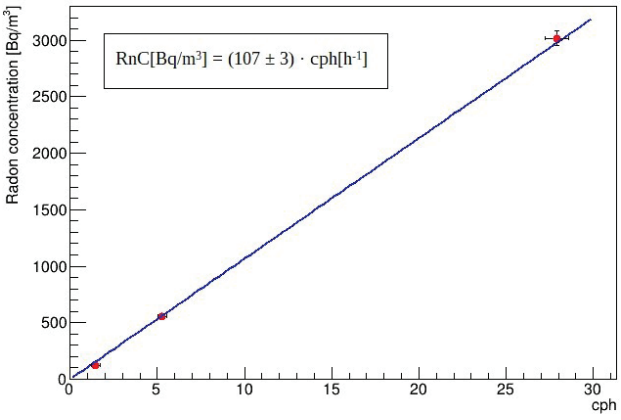

Fig. 9. Radon sensitivity of the first prototype.

Radon measurements

In order to acquire a radon spectrum, natural rock samples and the first prototype were placed inside the light-tight box. The spectrum was acquired operating the detector for 172,800 s. As is shown in Fig. 7, the alpha peaks from the decay of ^{218}Po and ^{214}Po can be clearly distinguished. At lower energies, it is evident the contribution of ^{222}Rn: a continuous spectrum with an end point of approximately 5.75 MeV. This measurement allowed to set the discrimination threshold at a corresponding energy of about 5.75 MeV in order to reject

Fig. 11. Plastic case prototype.

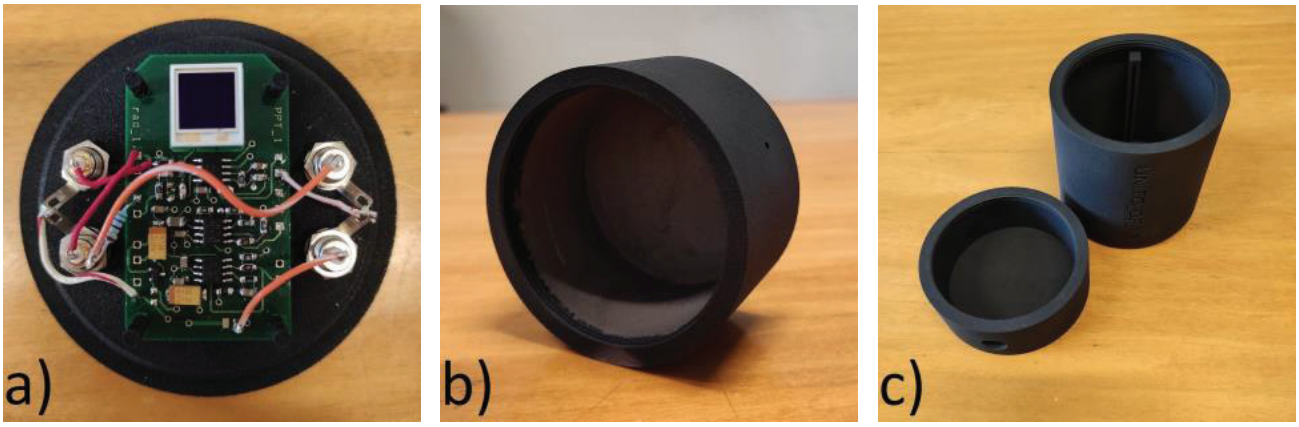

Fig. 10. Plastic case components. (a) PCB support; (b) diffusion passive chamber; (c) battery holder and bottom cap.

light and electronic noise and signals coming from alpha particles not belonging to ^{222}Rn and ^{220}Rn short life daughters.

Radon sensitivity assessment

The system was tested in laboratory conditions exposing both the first prototype and a calibrated commercial radon detector (RAD7 Durridge Inc.) to rock samples (Fig. 8). Three different configurations were tested, changing the number of rocks inside the metal box and the closing system. The count rates from the prototype, acquired using a digital panel counter (Trumeter HED 261-T) (14), are normalized and summarized in Table 2 and compared with the radon concentration (Bq m^{-3}) measured by RAD7. The prototype sensitivity of 107 ± 3 Bq/cph was obtained from the linear regression through the origin of the experimental data as displayed in Fig. 9. In terms of accuracy, this means about 20% after 1-day exposure and less than 10% for 1-week exposure at 100 Bq m^{-3}. These characteristics, sensitivity, and accuracy imply that the monitor is mainly suited for long-term (e.g. days) indoor measurements.

Final prototype

A 3d-print plastic case prototype was designed and realized using black PA12 (polyamide 12) for light shielding in order to host the whole system. The plastic case, as is shown in Fig. 10, is made up of four parts: the diffusion passive chamber (45 mm), the PCB support (26 mm), the battery holder (74 mm), and the bottom cap (30 mm). The device assembly has a diameter of 80 mm and a total height of 154 mm as shown in Fig. 11. Both the inside of the expansion chamber and the board support were painted with conductive paint for the electromagnetic shielding. The top portion of the case is provided with ventilation holes that allow the air to flow inside the diffusion passive chamber, but dust and debris particles are kept out by the presence of paper filters. Below that, there is the detector support, the related PCB and holes for lemo connections. One of the main features of the detector case is the possibility to operate the prototype with batteries or with a power supply using a specific hole on the bottom cap.

Conclusions

A continuous radon monitor based on Si PIN photodiode and a dedicated low power consumption electronic chain was designed and realized. The device allows both to acquire the spectrum of the incoming alpha particles using an external MCA or to count the digital signals using an external counter.

In order to verify the linearity and the performance of the spectroscopic chain, a mixed alpha calibration source was used. A first radon spectrum was acquired using rocks as radon sources. The detector sensitivity (in terms of counts per hour/Bq m^{-3}) was estimated by comparing it to a commercial detector. The final configuration including a new detector housing has been already designed and 3d printed. In the future, the prototype will be equipped with environmental sensors (temperature, pressure and relative humidity (RH)), an internal clock, a data storage, and transfer features (SD card slot and USB port) using an Arduino board or integrating a microcontroller (PIC 16LF19155).

The radon sensitivity of the final detector configuration will be assessed in a radon chamber. Furthermore, the device will be tested to define the sensitivity to ^{220}Rn.

Finally, a network of continuous radon monitor will be realized in order to monitor the radon concentration simultaneously in several Torino University workplaces.

Conflict of interest and funding

The authors declare no potential conflicts of interest. This work was financially supported by the Physics Department of the University of Torino.

References

1. Duggal V, Sharma S, Mehra R. Risk assessment of radon in drinking water in Khetri Copper Belt of Rajasthan, India. Chemosphere 2020; 239: 124782. doi: 10.1016/j.chemosphere.2019.124782
2. Appleton JD. Radon: sources, health risks, and hazard mapping. Ambio 2007; 36(1): 85–9. doi: 10.1579/0044-7447(2007)36[85:RSHRAH]2.0.CO;2
3. ICRP. Radiological protection against radon exposure. ICRP publication 126. Ann ICRP 2014; 43(3): 5–73. doi: 10.1177/0146645314542212
4. International Agency for Research on Cancer. Man-made mineral fibres and radon. IARC monographs on the evaluation of carcinogenic risks to humans vol. 43. Lyon: IARC; 1998.
5. World Health Organization. WHO handbook on indoor radon: a public health perspective. Geneva, Switzerland: World Health Organization; 2009. Available from: http://apps.who.int/iris/bitstream/handle/10665/44149/9789241547673_eng.pdf?sequence=1 [cited 29 June 2022].
6. Council Directive 2013/59/Euratom of 5 December 2013 laying down basic safety standards for protection against the dangers arising from exposure to ionising radiation, and repealing Directives 89/618/Euratom, 90/641/Euratom, 96/29/Euratom, 97/43/Euratom and 2003/122/Euratom. OJ L13; 2014; 1–73.
7. DURRIDGE Company Inc. RAD7 electronic radon detector user manual. Billerica, MA; 2022. Available from: https://durridge.com/documentation/RAD7%20Manual.pdf [cited 29 June 2022].
8. Si PIN photodiode, S3590-09 2020. Available from: https://www.hamamatsu.com/ content/dam/hamamatsu-photonics/sites/documents/99_SALES_LIBRARY/ssd/s3590-08_etc_kpin1052e.pdf [cited 29 June 2022].
9. Elísio S, Peralta L. Development of a low-cost monitor for radon detection in air. Nucl Instrum Methods Phys Res A: Accel

Spectrom Detect Assoc Equip 2020; 969: 164033. doi: 10.1016/j.nima.2020.164033
10. Gugliermetti L, Lepore L, Remetti R, Tosti MC. Alpha spectrometry with the inexpensive open-source detector Alphaino. Nucl Instrum Methods Phys Res A: Accel Spectrom Detect Assoc Equip 2019; 928: 13–19. doi: 10.1016/j.nima.2019.03.018
11. Amptek. Available from: https://www.amptek.com/-/media/ametekamptek/documents/resources/retired/mca8000a.pdf?la=en&revision=063c3df7-e723-4e9c-a9c9-a40ec176e4a2&hash=73C9143CCC7E5BB4DA70A3562F24BCB5 [cited 29 June 2022].
12. Eckert & Ziegler. Alpha spectroscopy sources. Available from: https://www.ezag.com/home/products/isotope_products/isotrak_calibration_sources/reference_sources/alpha_spectroscopy_sources/ [cited 29 June 2022].
13. National Institute of Standards and Technology. Available from: https://www.nist.gov/pml/radiation-dosimetry-data [cited 29 June 2022].
14. Trumeter. Available from: https://www.trumeter.com/product/hed251-hed261/ [cited 29 June 2022].

***Lorenzo Visca**

Physics Department of the University of Torino
via P. Giuria 1, 10125 Torino, Italy
Email: lorenzo.visca@unito.it